SKB

TECHNICAL REPORT 91-19

NEAR21 – A near field radionuclide migration code for use with the PROPER package

Sven Norman[1], Nils Kjellbert[2]

[1] Starprog AB
[2] SKB AB

April 1991

SVENSK KÄRNBRÄNSLEHANTERING AB
SWEDISH NUCLEAR FUEL AND WASTE MANAGEMENT CO

BOX 5864 S-102 48 STOCKHOLM

TEL 08-665 28 00 TELEX 13108 SKB S
TELEFAX 08-661 57 19

NEAR21 - A NEAR FIELD RADIONUCLIDE MIGRATION CODE FOR USE WITH THE PROPER PACKAGE

Sven Norman[1], Nils Kjellbert[2]

1 Starprog AB
2 SKB AB

April 1991

NEAR21 -

A Near Field Radionuclide Migration Code for use with the PROPER Package

Sven Norman
Starprog AB

Nils Kjellbert
SKB AB

April 1991

ABSTRACT

The near field radionuclide migration computer code NEAR21 has been developed as a submodel of the probabilistic package PROPER, and can be considered a PROPER version of the near field models used in the KBS-3 study.

NEAR21 computes the migration rates of radionuclide chains from the near field of one KBS-3 canister. Diffusive transport, canister corrosion, fuel matrix dissolution, solubility limitations under oxidizing and reducing conditions, washout of instantly released portions of the inventories and chain decay are all taken into account.

1. INTRODUCTION

The purpose of the PROPER code package is to provide the performance analyst with a computerized methodology that enables him/her to study the propagation of parameter uncertainties in performance-assessment-related model calculations.

The core of the PROPER package is the Monitor that is used to interconnect the desired submodels, selected from a library at runtime, and to propagate the input parameter uncertainties to find the associated uncertainties in the results, cf. Figure 1.1. This is accomplished without any intervention in the source code of the Monitor or the submodels. The submodels typically deal with groundwater flow and radionuclide migration.

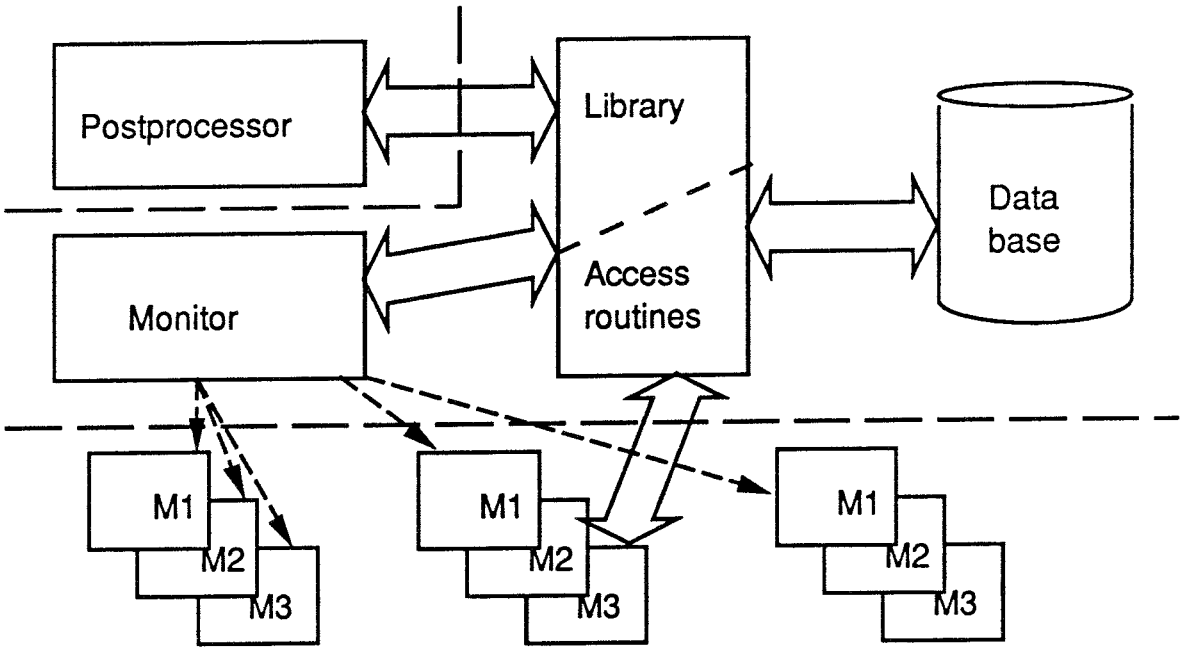

Figure 1.1
Schematic illustration of the function of PROPER

The numerical integration method used in PROPER is a Monte Carlo procedure using repeated sampling of parameter values.

The PROPER Monitor only collects crude statistics. Further evaluation must be carried out using a suitable post-processor.

The Monte Carlo approach requires that submodels are simplified and/or use very fast numerical algorithms.

The present report presents a submodel designed to calculate the rate of radionuclide transport from the near field of one KBS-3-design canister for spent fuel. It is based mainly on the near field model that was used in the KBS-2 and KBS-3 studies [1-1, 1-2] and on work that was reported with those studies.

The submodel, named NEAR21, represents a further development of the zero:th generation near field model NEAR20 which did not treat radionuclide chain decay, and which used nuclide-wise solubilities. NEAR21 is capable of handling chain decay and distributes element-wise solubilities among the different isotopes.

NEAR21 is coded in FORTRAN77 and was produced in accordance with the PROPER standard software engineering procedures.

The following chapters contain descriptions of the basic model (Chapter 2), the method for numerical solution (Chapter 3), the inputs to and outputs from NEAR21 (Chapter 4) and a test example (Chapter 5).

2. BASIC MODEL

2.1 General Assumptions

Figure 2.1 below shows "the artists impression" of a KBS-3 type copper canister for spent LWR fuel emplaced in its hole in the bedrock. The canister is surrounded by highly compacted bentonite.

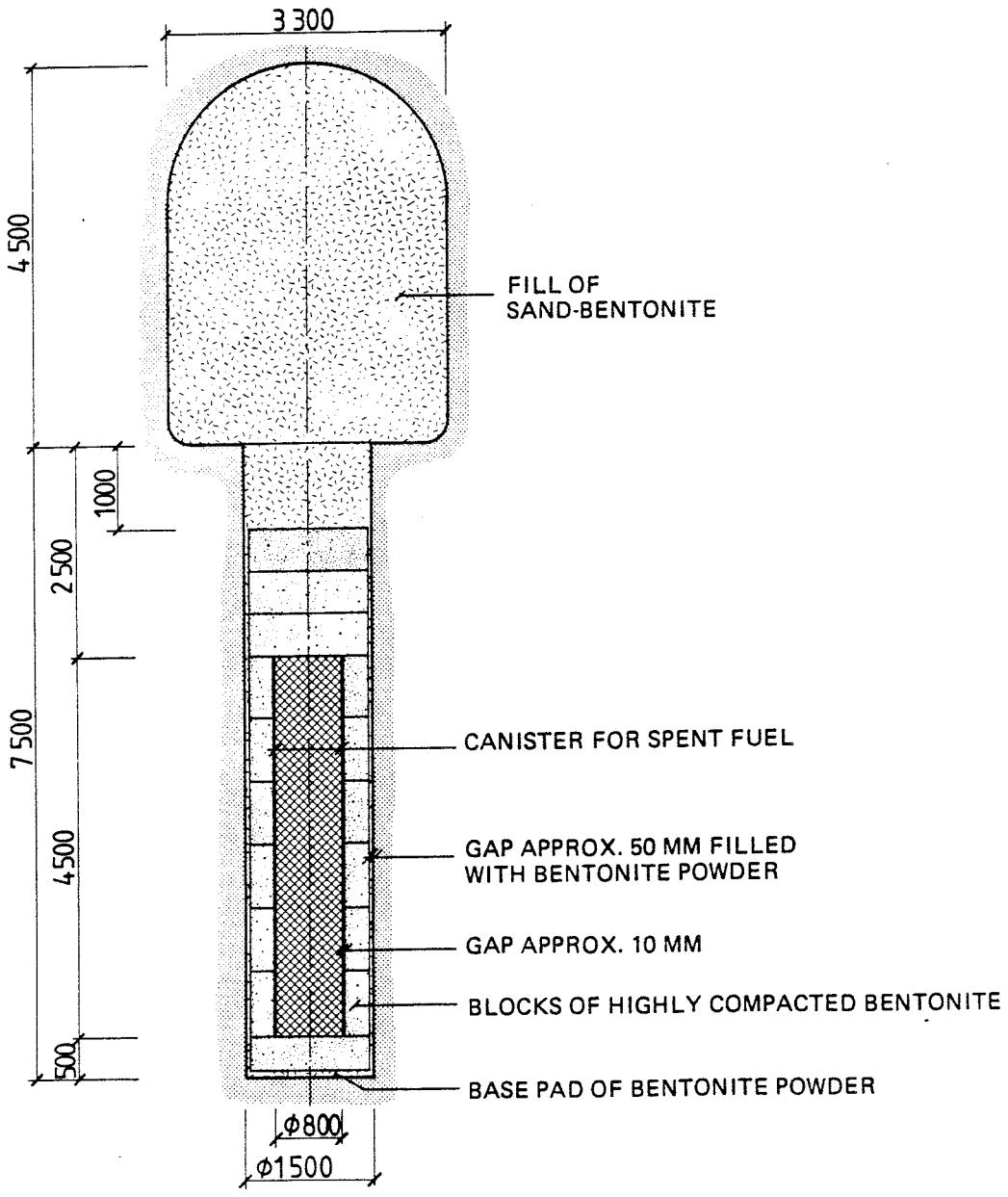

Figure 2.1
Deposition hole with canister and buffer material and with backfill in storage tunnel.

Figure 2.2 shows the schematic picture of the canister that forms the basis of the near field model.

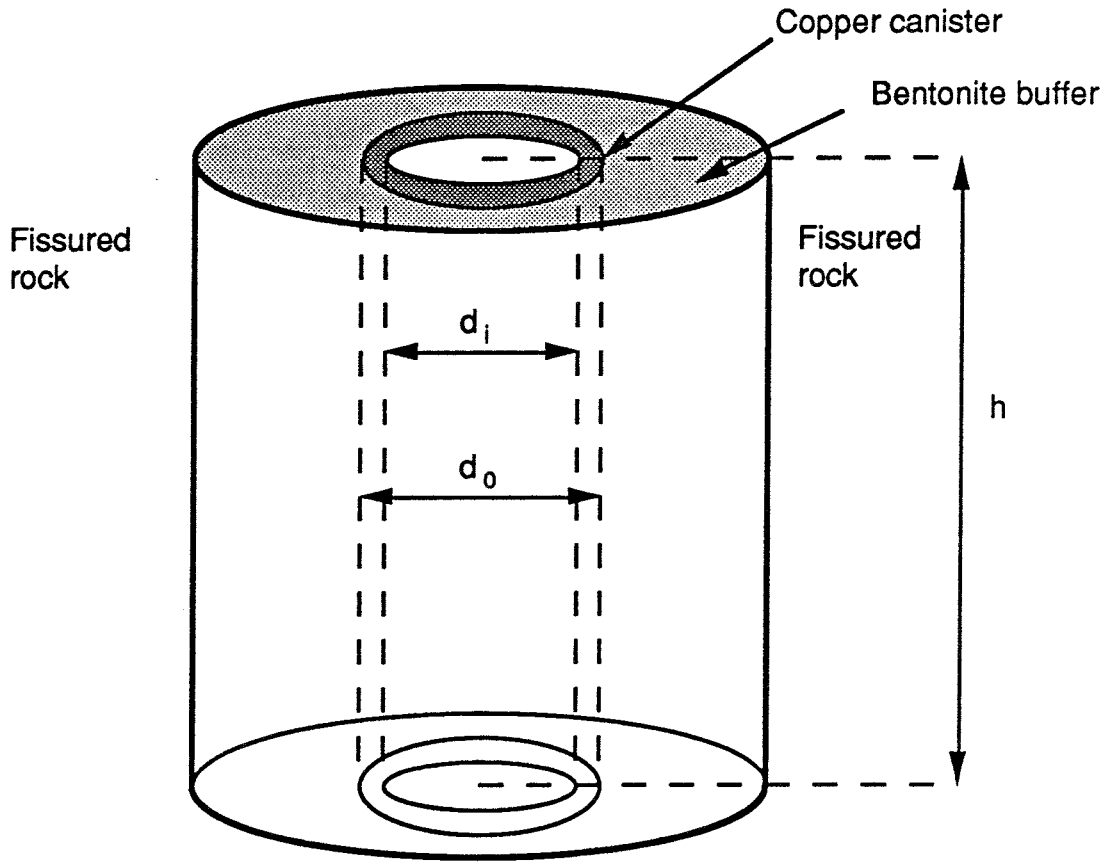

Figure 2.2
Schematic picture of KBS-3-type canister for spent fuel.The spent fuel is surrounded by a copper canister and a bentonite buffer.

In the present model, corrosion caused by sulphide is assumed to be the only important failure mode of the canister. As long as the canister remains intact there is no leakage of radionuclides from the near field.

After the canister is penetrated, radiolysis is assumed to cause oxidizing conditions in the immediate vicinity of the canister whereas reducing conditions are assumed to prevail at the outskirts of the near field. The basic assumption is that oxidizing conditions prevail where mass transfer resistance is dominated by diffusion.

2.2 Mass Transfer Resistance

2.2.1 Specific Assumptions

Steady-state conditions are assumed for both the inward transport of corrodants and the outward transport of radionuclides once the canister is penetrated. The time constants for the transient phase of the mass transfer are short compared to the durability of the copper and the life times of the radionuclides that have to be considered, which justifies this particular assumption.

2.2.2 Diffusive Transport

For the fuel matrix and the oxidizing region diffusion is assumed to determine the rate of mass transfer.The kind of problem to be solved is illustrated in Figure 2.3. The figure and the following presentation actually describes the outward transport problem. The mass transfer resistance in the inward direction is of course the same.

The mass transfer is driven by differences in chemical potentials (here: = intrinsic phase average concentration) and the transfer rate can be expressed as

$$J = kA\Delta C \quad [MT^{-1}] \tag{2.1}$$

where

ΔC = characteristic concentration difference $[ML^{-3}]$,

A = characteristic area $[L^{2}]$,

k = effective mass transfer coefficient $[LT^{-1}]$.

Hence, the steady-state transport resistance due to diffusion can be described by a single number: the product kA has the dimensions $[L^{3}T^{-1}]$ and can be interpreted as an equivalent flow rate Q_{eq} that enters the near field with one concentration and leaves it with another [2-1]:

$$Q_{eq} = kA \quad [L^3T^{-1}]. \tag{2.2}$$

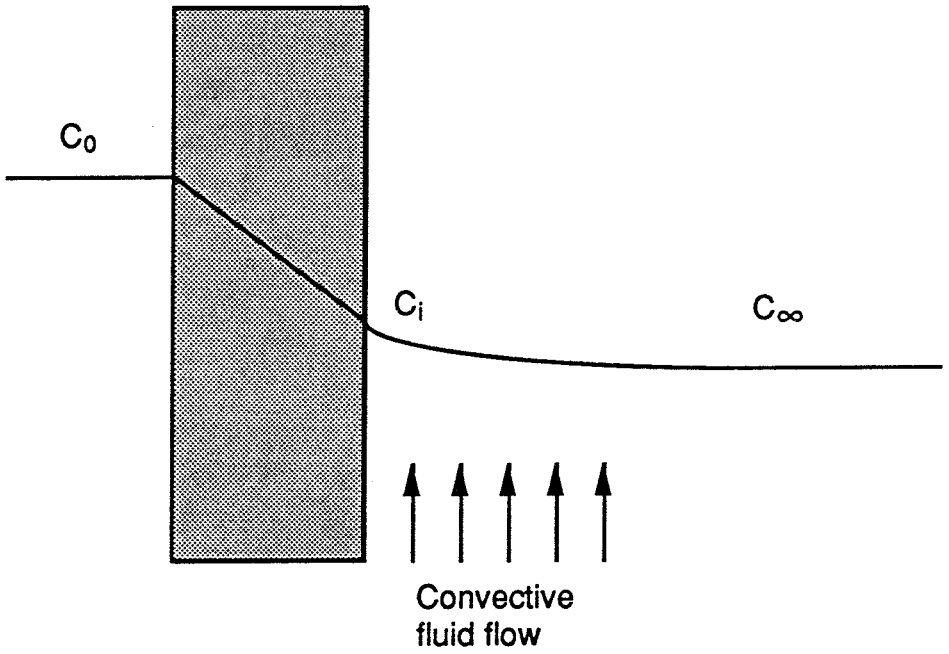

Figure 2.3
Illustration of mass transfer problem showing, schematically, a small piece of the clay barrier and the surrounding rock. C_0 is the concentration insisde the clay, C_i is the concentration at the clay / rock interface and C_∞ is the ambient concentration.

The transfer domain is split up into two sub-domains, L and V corresponding to the clay barrier and the rock respectively , each having constant properties:

$$C_\infty = 0 \quad \Rightarrow \quad J = kAC_0 = k_L A_L(C_0 - C_i) = k_V A_V C_i \tag{2.3}$$

or

$$\frac{1}{kA} = \frac{1}{k_L A_L} + \frac{1}{k_V A_V} \tag{2.4}$$

which allows the overall transfer coefficient to be computed from the coefficients of the sub-domains.

For the diffusion through the clay we write using Ficks first law:

$$J = A_L j_L = - A_L D_e \frac{C_i - C_0}{\Delta r_L} \quad \Rightarrow \quad k_L A_L = D_e \frac{A_L}{\Delta r_L} \qquad (2.5)$$

where

A_L = effective surface area [L^2]
C_0 = concentration inside barriers [ML^{-3}],
C_i = concentration at interface between buffer and rock [ML^{-3}],
D_e = effective molecular/ionic diffusivity in the clay [L^2T^{-1}],
Δr_L = effective diffusion length [L].

Neretnieks [2-2] has devised a procedure to compute the ratio $A_L/\Delta r_L$ assuming that the area available to convective fluid flow at the outer boundary of the clay determines the resistance to transfer *out of* the clay barrier. The procedure uses the exact solution of the steady state 2-D diffusion equation for a sector of the clay barrier representing half the fissure spacing which allows reflexive boundary conditions to be used. The result is written as

$$\frac{A_L}{\Delta r_L} = \frac{\varepsilon_f A_{out}}{F_{x0}} \qquad (2.6)$$

where $F_{x0}(a, b, d)$ is an effective diffusion length function and where

ε_f = flow porosity outside buffer [−],
A_{out} = entire outside surface area of buffer [L^2],
b = half fissure aperture [L],
a = half fissure spacing [L],

$$d = \frac{d_h - d_o}{2} \quad [L]$$

(d_h diameter of deposition hole, d_o = outer diameter of canister).

The effective diffusion length function is a very complicated expression and a response -function type replacement has been estimated by Neretnieks [2-2] using a number of fracture spacings, fracture apertures and barrier thicknesses and found to be represented well by the expression

$$F_{x0} = b\,(1 - 1.35 \cdot \lg\frac{b}{a} + 1.6 \cdot \lg\frac{d}{a}) \qquad (2.7)$$

for $10^{-6} < b/a < 10^{-1}$ and $0.03 < d/a < 1$.

To tackle the sub-domain where the Darcy flow is assumed to control the diffusion rates, an approach based on penetration theory [2-3] is employed. The idea is to solve the steady state diffusive-convective transport problem by solving the transient diffusive problem in a quasi-stationary manner using Ficks second law . The time-dependent equation is solved for the so called penetration period, during which no flow is assumed, only diffusion. After each period, the contaminated fluid is assumed to be momentarily replaced at the interface with fresh fluid having the ambient concentration.

Neglecting end effects the appropriate equations and boundary conditions are[1]:

$$\frac{\partial C}{\partial t} = D_V \frac{\partial^2 C}{\partial x^2} \qquad (2.8)$$

$$t = 0, \quad C = 0$$

---

[1]The concentration will typically drop by 95 percent within a few decimeters from the clay / rock interface, which should justify the use of a flat geometry instead of a cylindrical one.

$$x = 0, \quad C = C_i \tag{2.9}$$

$$x \to \infty, C = 0$$

where

D_V = diffusion constant in groundwater [L^2T^{-1}]
x = radial distance from the clay/rock interface [L]

giving the outward transfer rate

$$J = \varepsilon_f A_{out} \frac{1}{t_k} \int_0^{t_k} - D_V \left(\frac{\partial C}{\partial x} \right)_{x=0} dt \tag{2.10}$$

where t_k is the penetration period. In this case, the penetration period is taken to be the time for the local, undisturbed flow to pass the deposition hole with its canister, which is along the lines of [2-3]:

$$t_k = \varepsilon_f \min \left\{ \frac{d_h}{|U_{0x}|}, \frac{h}{|U_{0z}|} \right\} \tag{2.11}$$

where

ε_f = flow porosity outside buffer [–],
d_h = diameter of deposition hole [L],
h = height of canister [L],
U_{0x} = undisturbed horiz. Darcy velocity outside canister [LT^{-1}],
U_{0z} = undisturbed vertical Darcy velocity outside canister [LT^{-1}].

The differential equation (2.8) - (2.9) is solved in Appendix A. The solution gives

$$J = \varepsilon_f A_{out}\left(\frac{4D_V}{\pi t_k}\right)^{1/2} C_i \Rightarrow k_V A_V = \varepsilon_f A_{out}\left(\frac{4D_V}{\pi t_k}\right)^{1/2}. \qquad (2.12)$$

Exactly the same expression can be derived taking using a discrete description of the fissured rock where the fractures are taken into account explicitly [2-4].

2.2.3 Advective Transport

At the outskirts of the near field the migration of radionuclides is driven by advection. The advective transport can also be described by a single number, referred to as Q_{red} in the sequel [2-1]. The volume available for a solubility limited species at the redox front is assumed to be determined by the groundwater flow over a cross section equivalent to that of the deposition hole perpendicularly to the flow:

$$Q_{red} = \frac{\pi d_h^{\,2}}{4}|U_{0z}| + h d_h |U_{0x}| \quad [\mathrm{L^3T^{-1}}] \qquad (2.13)$$

where

d_h = diameter of deposition hole [L],
h = height of canister [L],
U_{0x} = undisturbed horiz Darcy velocity outside canister [$\mathrm{LT^{-1}}$],
U_{0z} = undisturbed vertical Darcy velocity outside canister [$\mathrm{LT^{-1}}$].

2.3 Canister Corrosion

The calculation of the time to canister penetration is easily achieved given the concentration of corrodant in water and the amount of copper that has to be corroded away. The overall corrosion process is such that two atoms of copper reacts with one atom of sulphide, to produce the corrosion product Cu_2S [2-5]. The time to penetration is thus

$$T_{break} = \frac{N_{cu}}{2Q_{eq}C_{HS^-}} \quad [\mathrm{T}] \tag{2.14}$$

where

N_{Cu} = amount of copper corroded at penetration [M],
C_{HS^-} = concentration of sulphide in groundwater [ML^{-3}].

The kinetics are assumed to be fast so that the corrosion can be assumed to be transport-controlled.

The amount of copper that has to be corroded away is not necessarily the entire canister. Pit corrosion cannot be excluded [2-5]. In order to take the possibility of pitting into account a pitting factor is introduced, defined as the ratio between the actual maximal penetration depth and the penetration depth obtained if the corrosion were uniformly distributed.

The oxygen present in the buffer and backfill immediately after repository closure must also be assumed to be able to consume some of the copper in the canister. To take this into account, an "initial penetration" is introduced so that the actual amount of copper that is left to be corroded away by the sulphide is

$$N_{Cu} = \frac{\rho_{Cu}}{M_{Cu}} \pi h \left[\left(\frac{d_{init}}{2} \right)^2 - \left(\frac{d_{break}}{2} \right)^2 \right] \tag{2.15}$$

where

ρ_{Cu} = density of copper [ML^{3}],
M_{Cu} = molar weight of copper [–],
h = height of canister [L],

and where

$$d_{init} = d_o - 2p_0$$

$$d_{break} = d_i + (d_o - d_i)\left(\frac{p_f - 1}{p_f}\right) \tag{2.16}$$

where

d_o = outer diameter of canister [L],
d_i = inner diameter of canister [L],
p_0 = initial uniform penetration [L],
p_f = pitting factor [–].

Only the mantle of the canister has been included which is slightly conservative.

All the fuel is assumed to be exposed to the groundwater as soon as the canister is penetrated. Any mass transfer resistance in the pit or due to corrosion products is neglected.

2.4 Radionuclide Mass Balance Relations

2.4.1 Specific Assumptions

In the unperturbed rock conditions are expected to be chemically reducing. After the canister has been penetrated, conditions are expected to change in its vicinity due to radiolysis, creating a zone with oxidizing conditions. The interface between the the two is expected to be narrow creating a well defined boundary usually referred to as the redox front.

The different elements present in the spent fuel are assumed to be evenly distributed in the matrix and they cannot leach into the water without dissolution of the corresponding matrix as well. There is a small number of elements for which this is not true; on the contrary it is known that elements such as Cesium and Iodine are to some extent concentrated on the surface of the fuel, or in the gap between the cladding and the fuel.

NEAR21 is designed to take fuel matrix dissolution, precipitation at oxidizing and reducing conditions and leaching and washout of the fuel-to-clad gap inventories into account. For that purpose, the near field of

the canister is split up into control volumes, see Figure 2.4. For each control volume, a mass balance is set up according to the basic principle

IN + PRODUCED = OUT + ACCUMULATED

or

ACCUMULATED = (IN-OUT) + PRODUCED

which is reflected in the equations below.

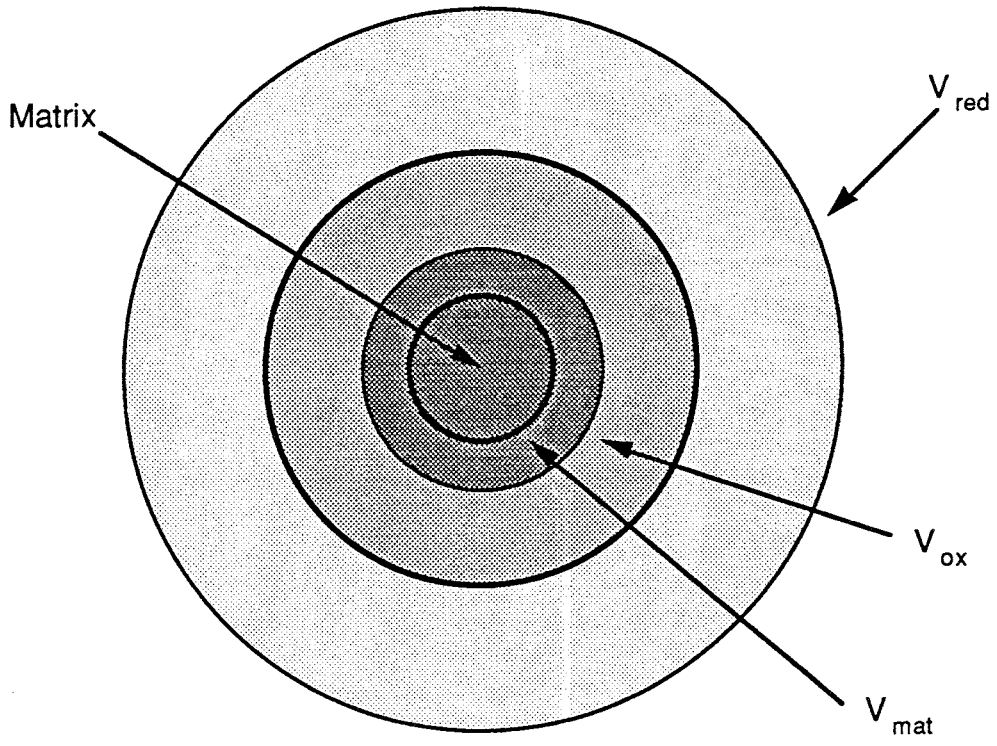

Figure 2.4
Control volumes in the near field model.

It is also assumed that the residence time for any species in dissolved form in any of the regions is short compared to other time constants in the system, and in any case negigible compared to the residence times for species in solid form, the latter being the only time factors taken into account (material is allowed to accumulate in solid form only).

2.4.2 Fuel Matrix

It is assumed that in a small volume denoted V_{mat} surrounding the fuel the concentration of Uranium, that is ^{238}U, is given precisely by the solubility of Uranium under oxidizing conditions $C_{s,ox,U}$. The different chemical elements contained in the fuel are dissolved proportionally to the dissolution of Uranium (with the exception of the gap inventories) giving a concentration in the outermost layer of the matrix:

$$C_{mat,i}(t) = \frac{C_{s,ox,U} V_{mat}}{N_{mat,U}} \frac{N_{mat,i}}{V_{mat}} = \frac{N_{mat,i}}{N_{mat,U}} C_{s,ox,U} \quad [ML^{-3}] \quad (2.17)$$

where $N_{mat,i}(t)$ is the amount of nuclide i in the matrix [M], where t is time [T] elapsed from the time of canister breakthrough T_{break} and U stands for ^{238}U.

The outward migration rate of nuclide i from the matrix resulting from these concentrations then becomes $Q_{eq} C_{mat,i}$ and the mass balance for the matrix can be written as

$$\frac{dN_{mat,i}}{dt} = - Q_{eq} C_{mat,i} + (\Lambda \mathbf{N}_{mat})_i \quad (2.18)$$

where $\mathbf{N}_{mat}$ is the vector whose i:th component is $N_{mat,i}$ and Λ is the decay matrix .

The solubility restriction is introduced by the requirement

$$\sum_{j \in J(i)} C_{mat,j} \geq C_{s,ox,J(i)} \Rightarrow \text{precipitation occurs} \quad (2.19)$$

where $C_{s,ox,J(i)}$ denotes the solubility of the chemical substance $J(i)$ under oxidizing conditions, and where $J(i)$ denotes the set of all

nuclides, or rather the set of all numbers associated with a nuclide, such that $j \in J(i) = J(j)$ implies that i and j are isotopes of the same chemical element.

2.4.3 Oxidizing Region

Now if (2.19) prevails, substance in precipitated form will accumulate in a zone just outside the matrix or for the sake of modeling in a region V_{ox} sharing boundary with V_{mat} ,see Figure 2.4. The mixture entering V_{ox} , thus has concentration $C_{mat,i}$.

Let us denote the amount of nuclide i precipitated in V_{ox} by $N_{ox,i}(t)$ and $C_{ox,i}(t)$ is the concentration of nuclide i in the mixture leaving V_{ox}. When there is no precipitate present i.e when

$$\sum_{j \in J(i)} N_{ox,j} = 0.$$

the output concentration $C_{ox,i}(t)$ is taken to be

$$C_{ox,i}(t) = \min\left\{ C_{mat,i},\ \frac{C_{s,ox,J(i)} C_{mat,i}}{\sum_{j \in J(i)} C_{mat,j}} \right\} \tag{2.20}$$

thus ensuring that the concentration of the chemical substance $J(i)$ leaving V_{ox} does not exceed the solubility limit $C_{s,ox,J(i)}$ .This results in a mass balance relation

$$\frac{dN_{ox,i}}{dt} = Q_{eq}(C_{mat,i} - C_{ox,i}) + (\Lambda \mathbf{N}_{ox})_i$$

$$= Q_{eq} \frac{C_{mat,i}}{\sum_{j \in J(i)} C_{mat,j}} \left(\sum_{j \in J(i)} C_{mat} - C_{s,ox,J(i)} \right)^{+} + (\Lambda N_{ox})_i . \quad (2.21)$$

Here superindex + is a general notation meaning

$$f^{+} = \max(f, 0) .$$

Note that this is a model for the initial growth of $N_{ox,i}(t)$ which is onset only when

$$\sum_{j \in J(i)} C_{mat} - C_{s,ox,J(i)} > 0 .$$

When , on the other hand, a precipitate is present, i.e. when

$$\sum_{j \in J(i)} N_{ox,j} > 0$$

it is assumed that the mixture leaving V_{ox} is in chemical equilibrium with the precipitate, that is we replace (2.20) with

$$C_{ox,i}(t) = \frac{C_{s,ox,J(i)} N_{ox,i}}{\sum_{j \in J(i)} N_{ox,j}} \quad (2.22)$$

and the mass balance relation correspondingly.

The release of the fuel-to-clad gap inventories is modeled in the simplest possible way by just placing the part of the inventory which is concentrated at the surface of the fuel as a initial value for the variable N_{ox} .

2.4.4 Reducing Region

For the sake of modeling V_{red} is a volume including the redox front immediately outside its inner boundary, cf. Figure 2.4. Moreover since the redox front is assumed to lie beyond the buffer and therefore also beyond the region where diffusion dominates the transport resistance we adopt the model that the radionuclides at the redox front are carried convectively by the the actual water flow through the redox front, Q_{red}, [2 - 1]. Hence by mass conservation

$$Q_{eq} C_{ox,i} = Q_{red} C_{ox,i}^{in} \tag{2.23}$$

where $C_{ox,i}^{in}(t)$ is the concentration of nuclide i in the mixture passing through the inner boundary of V_{red}. This leads to the introduction of a dilution factor $S = Q_{eq}/Q_{red}$ which enables us to compute the ingoing concentration $C_{ox,i}^{in}$ in terms of $C_{ox,i}$ Now precisely the same analysis is done as for the oxidizing region with $N_{red,i}(t)$ denoting the amount of nuclide i precipitated at the redox front, that is in V_{red}, and $C_{red,i}$ is the concentration of nuclide i in the mixture leaving V_{red}. We obtain the mass balance equations

$$\frac{dN_{red,i}}{dt} = Q_{red}(S\, C_{ox,i} - C_{red,i}) + (\Lambda \mathbf{N}_{red})_i \tag{2.24}$$

where

$$C_{red,i}(t) = \min\left\{ S\, C_{ox,i},\ \frac{C_{s,red,J(i)} C_{ox,i}}{\sum_{j \in J(i)} C_{ox,j}} \right\} \tag{2.25}$$

when

$$\sum_{j \in J(i)} N_{red,j} = 0$$

and

$$C_{red,i}(t) = \frac{C_{s,red,J(i)} N_{red,i}}{\sum_{j \in J(i)} N_{red,j}} \tag{2.26}$$

when

$$\sum_{j \in J(i)} N_{red,j} > 0.$$

The outward migration rate of nuclide i from the near field is finally obtained as

$$J_i(t) = Q_{red} C_{red,i}(t) \quad [\mathrm{MT}^{-1}]. \tag{2.27}$$

3. NUMERICAL SOLUTION

Since the boundary conditions for $N_{ox,i}$ are homogeneous, i.e $N_{ox,i} = 0$ for all i at t = 0, the mass balance equation

$$\frac{dN_{ox,i}}{dt} = Q_{eq}(C_{mat,i} - \frac{C_{s,ox,J(i)}N_{ox,i}}{\sum_{j \in J(i)} N_{ox,j}}) + (\Lambda N_{ox})_i \qquad (3.1)$$

is singular and we can not rely on the usual theorems for existence and uniqueness. In fact it is easy to find examples on similar equations where the solutions are not unique, for instance take $\Lambda \equiv 0$ in the equations above. Then one easily shows that the resulting equation can be written as a system of linear differential equations with constant coefficients in the variables

$$\begin{cases} z_i = \dfrac{N_{ox,i}}{\sum_{j \in J(i)} N_{ox,j}} & \text{if } J(i) \neq \{i\} \\ z_i = N_{ox,i} & \text{if } J(i) = \{i\} \end{cases} \qquad (3.2)$$

It follows from the theory of ordinary differential equations that the solution of these equations is determined by the set of values $z_i(0)$. However these are not determined by the homogenous boundary conditions of $N_{ox,i}$ but rather , by appeal to l'Hospitals rule, by the set of values $N'_{ox,i}(0)$.

The derivatives of $N_{ox,i}$ at zero could be obtained from (2.21) leading to a non-standard overdetermined equation. The idea, however, is not to digress into existence theory: for differential equations the goal of the analysis is a numerical model for the near field. In this numerical model Equations (2.20)-(2.21) are used in the region where

$$\sum_{j \in J(i)} N_{ox,j} \leq \varepsilon$$

producing a starting point with

$$\sum_{j \in J(i)} N_{ox,j} > \varepsilon$$

for the differential equation (3.1) above. Here ε is a parameter chosen "sufficiently small".

The same scheme is used for the reducing region.

Equations (2.20)-(2.22) and (2.24)-(2.26) are first solved in order to obtain all the nuclide contents as a function of time. The resulting coupled set of equations have all the characteristics of a stiff system. In NEAR21, this system of equations is solved using the MOLCOL algorithm (MOLCOL = Modified One-Leg COLlocation) developed by. Lars Eriksson of Starprog AB and Prof. Germund Dahlquist of the Department of Numerical Analysis and Computing Science, Royal Institute of Technology

In the final step, Equation (2.27) is used to obtain the outward transport rate of each nuclide.

4. INPUTS AND OUTPUTS

Since NEAR21 is a PROPER submodel the input and output data must follow the format imposed by the PROPER Monitor.

In principle, NEAR21 demands the following INPUTS:

* From other models:
  - horizontal and vertical Darcy velocity of groundwater outside canister, U_{0x} and U_{0z} ,
* Sampled Parameters:
  - copper corrosion pitting factor, p_f ,
  - penetration from general corrosion at time zero, p_0,
  - concentration of sulphide in groundwater, C_{HS^-} ,
  - effective diffusion coefficient in clay buffer, D_e ,
  - fissure spacing outside buffer, $2a$,
  - half fissure aperture, b ,
  - diffusion coefficient in water, D_V ,
  - solubility concentration under oxidizing conditions (for each chemical element), $C_{s,ox,J}$,
  - solubility concentration under reducing conditions (for each chemical element), $C_{s,red,J}$,
  - fraction of inventory released instantly(for each instantly released nuclide).
* Other data:
  - dimensions of deposition hole and canister,

- data describing the decay chains, i e half lives etc,
- information on where to get radionuclide inventories at time of canister penetration,
- solver parameters (optional).

and returns the following OUTPUT time series:

- migration rate from canister for each nuclide.

The radionuclide inventories at the time of emplacement are read automatically by NEAR21 from two files created by the BATEMAN code. The names of those files must be given in the input data.

The density and molar weight of copper are automatically set to 8930 kg/m^3 and 0.063546 kg/mol respectively.

5. TEST EXAMPLE

To demonstrate the type of results obtained by the NEAR21 submodel, a single-realization test example was designed.

5.1 Input data

* Hydrological data:

  - Horizontal Darcy velocity: $3.0 \cdot 10^{-3}$ m/a
  - Vertical Darcy velocity: 0 m/a

* Sampled parameters:

  - Half fissure width: $5 \cdot 10^{-5}$ m
  - Effective diffusivity in buffer: $1.3 \cdot 10^{-3}$ m^2/a
  - Effective diffusivity in water: $6 \cdot 10^{-2}$ m^2/a
  - Pitting factor: 25
  - Penetration at time zero: 0.0023 m
  - Sulphide concentration: 0.015 mol/m^3
  - Fissure spacing: 1 m
  - Solubilities under oxidizing conditions (mol/m^3):

Uranium	1.513
Thorium	$1.739 \cdot 10^{-6}$
Neptunium	2.0
Others	high

- Solubilities under reducing conditions (mol/m^3):

Uranium	$2.0 \cdot 10^{-4}$
Thorium	$2.0 \cdot 10^{-7}$
Neptunium	$2.0 \cdot 10^{-6}$
Technetium	$2.0 \cdot 10^{-5}$

Others high

* Dimensions of canister and deposition hole:

- Height of canister 4.5 m
- Inner diameter of canister 0.68 m
- Outer diameter of canister 0.8 m
- Diameter of deposition hole 1.5 m

* Inventories at time zero (moles) from the BATEMAN files, and half lives:

- ^{229}Th	0.01362	7.3 kyrs
- ^{230}Th	0.3757	80 kyrs
- ^{232}Th	0.09914	14.1 Gyrs
- ^{233}U	0.324	159 kyrs
- ^{234}U	1.820	245 kyrs
- ^{235}U	65.96	704 Myrs
- ^{236}U	32.67	23.4 Myrs
- ^{238}U	5588	4.47 Gyrs
- ^{237}Np	12.57	2.14 Myrs

5.2 Output data

The following breakthrough curves were obtained

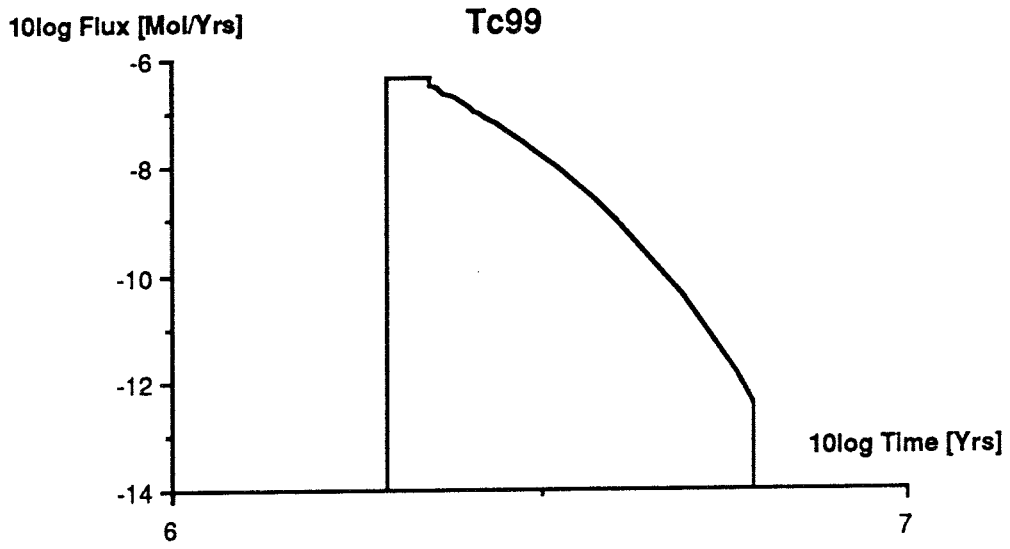

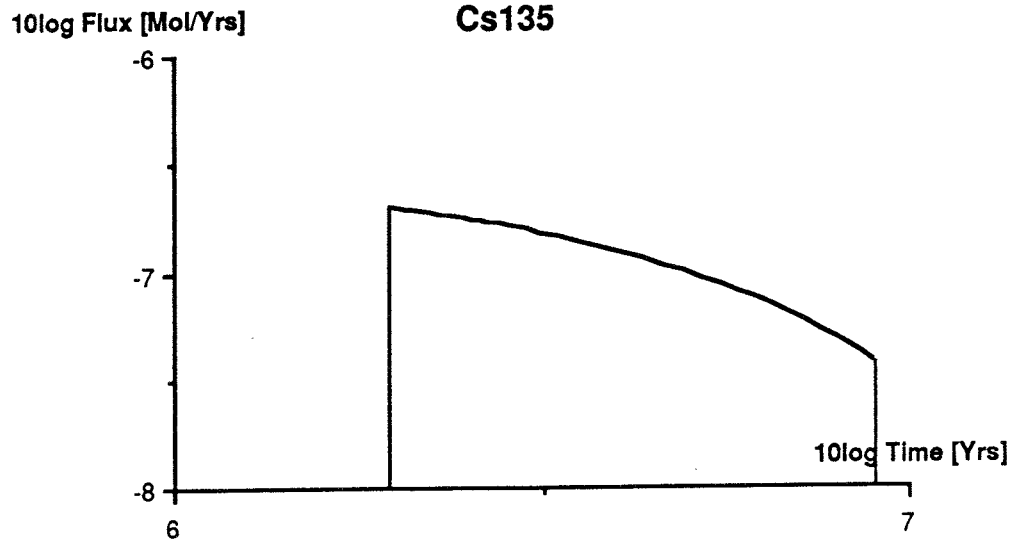

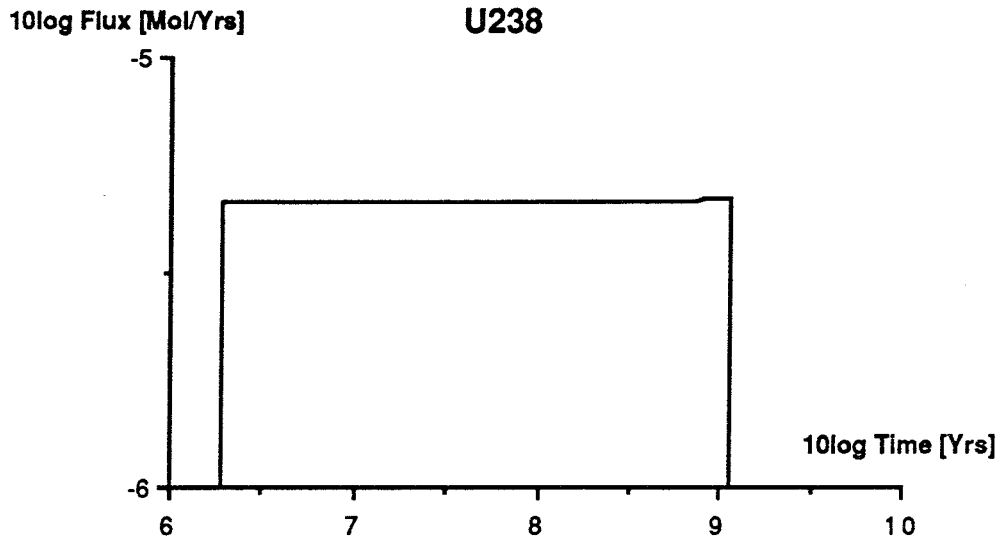
10log Flux [Mol/Yrs]
U238
-5
-6
6
7
8
9
10
10log Time [Yrs]

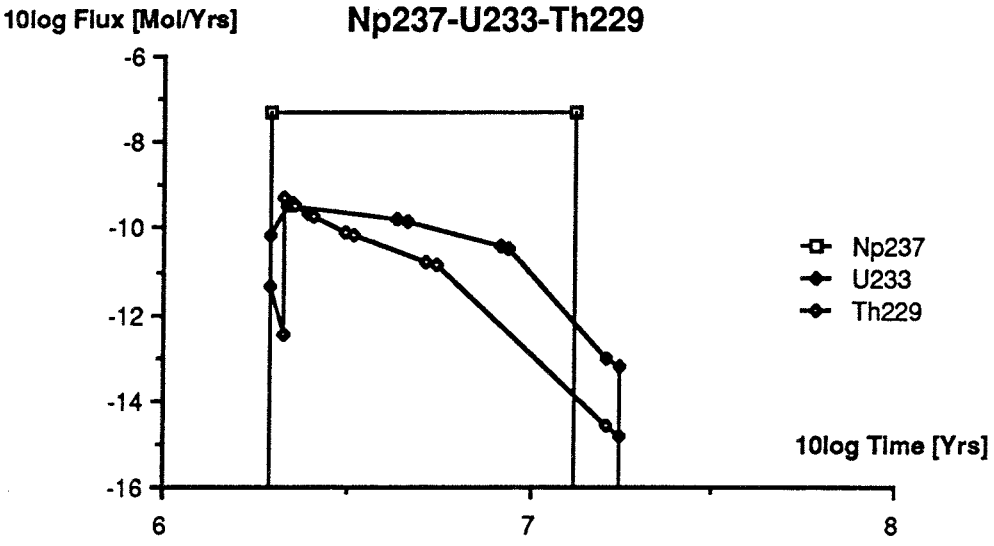
10log Flux [Mol/Yrs]
Np237-U233-Th229
-6
-8
-10
-12
-14
-16
6
7
8
Np237
U233
Th229
10log Time [Yrs]

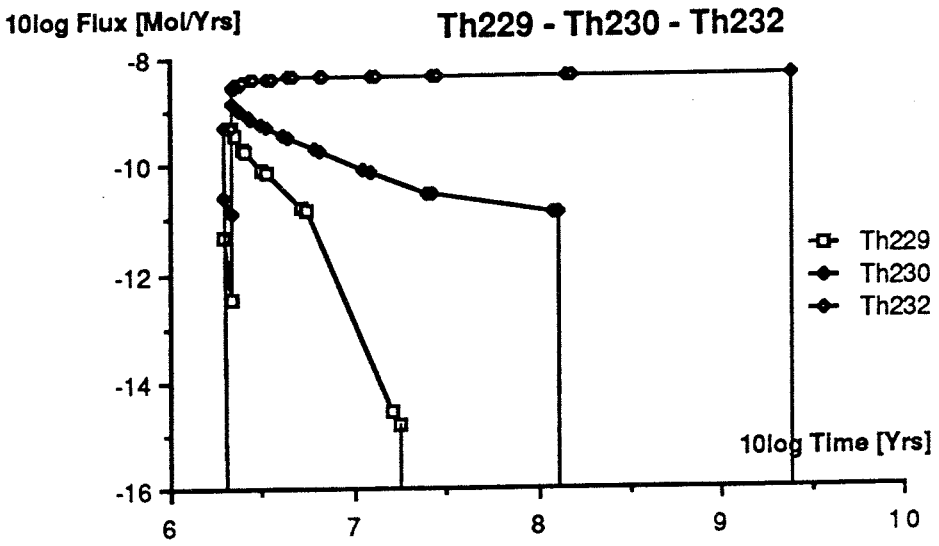
10log Flux [Mol/Yrs]
Th229 - Th230 - Th232
-8
-10
-12
-14
-16
6
7
8
9
10
Th229
Th230
Th232
10log Time [Yrs]

6. NOTATION

A = characteristic area [L^2],

k = effective mass transfer coefficient [LT^{-1}],

D_e = effective molecular/ionic diffusivity in the clay [L^2T^{-1}],

ε_f = flow porosity outside buffer [–],

A_{out} = entire outside surface area of buffer [L^2],

b = half fissure aperature [L],

a = half fissure spacing [L],

D_V = diffusion constant in groundwater [L^2T^{-1}],

d_h = diamter of deposition hole [L],

h = height of canister [L],

U_{0x} = undisturbed horiz. Darcy velocity outside canister [LT^{-1}],

U_{0z} = undisturbed vertical Darcy velocity outside [LT^{-1}],

C_{HS^-} = concentration of sulphide in groundwater [ML^{-3}],

ρ_{Cu} = density of copper [ML^3],

M_{Cu} = molar weight of copper [–],

d_o = outer diameter of canister [L],

d_i = inner diameter of cantister [L],

p_0 = initial uniform penetration [L],

p_f = pitting factor [–],

$C_{s,ox,U}$ = solubility of Uranium under oxidizing conditions,

$N_{mat,i}(t)$ = the amount of nuclide i in the matrix [M],

Λ = the decay matrix, i.e. $\frac{d}{dt}\mathbf{N} = \Lambda\mathbf{N}$, and $\mathbf{N}_{mat}$ is the vector whose i:th component is $N_{mat,i}$,

$C_{s,ox,J(i)}$ = the solubility of the chemical substance $J(i)$ under oxidizing conditions, where $J(i)$ denotes the set of all nuclides, or rather the set of all numbers associated with a nuclide, such that $j \in J(i)$ implies that i and j are isotopes of the same chemical element [ML^{-3}],

$C_{s,red,J(i)}$ = the solubility of the chemical substance $J(i)$ under oxidizing conditions,

$N_{ox,i}(t)$ = the amount of nuclide i precipitated in the control volume V_{ox} (see fig 2.4) [M],

$N_{red,i}(t)$ = the amount of nuclide i precipitated at the redox front [M],

$C_{mat,i}(t)$ = the concentration of nuclide i in the outermost layer of the matrix [ML^{-3}],

$C_{ox,i}(t)$ =the concentration of nuclide i in the mixture leaving the control volume V_{ox} (see fig 2.4) [ML^{-3}],

$C_{red,i}(t)$ =the concentration of nuclide i in the mixture leaving the nearfield [ML^{-3}].

REFERENCES

1-1 Handling and Final Storage of Unreprocessed Spent Nuclear Fuel. Projekt Kärnbränslesäkerhet, 1978.

1-2 Final Storage of Spent Nuclear Fuel - KBS-3. Swedish Nuclear Fuel Supply Co, 1983.

2-1 Final Storage of Spent Nuclear Fuel - KBS-3. III: Barriers. Swedish Nuclear Fuel Supply Co, 1983.

2-2 NERETNIEKS, I
Stationary Transport of Dissolved Species in the Backfill Surrounding a Waste Canister in Fissured Rock: Some Simple Analytical Solutions. Nuclear Technology **72**, pp 194-200 (1986).

2-3 HIGBIE, R
The Rate of Absorption of a Pure Gas into a Still Liquid during Short Periods of Exposure.
Trans AIChE **31**, pp 365-389 (1935).

2-4 ANDERSSON, G, RASMUSON, A, and NERETNIEKS, I
Migration Model for the Near Field: Final Report.
KBS Technical Report 82-24, Swedish Nuclear Fuel Supply Co, November 1982.

2-5 The Swedish Corrosion Research Institute and its Reference Group
Corrosion Resistance of a Copper Canister for Spent Nuclear Fuel.
KBS Technical Report 83-24, Swedish Nuclear Supply Co, April 1983

APPENDIX A: Solution of Transient Equation for One Penetration Period

To overall output rate is expressed as the mean of the output taken over the penetration period:

$$J = \varepsilon_f A_{out} \frac{1}{t_k} \int_0^{t_k} - D_V \left(\frac{\partial C}{\partial x} \right)_{x=0} dt . \qquad (A.1)$$

The time-dependent equation is:

$$\frac{\partial C}{\partial t} = D_V \frac{\partial^2 C}{\partial x^2} \qquad (A.2)$$

$$t = 0, \quad C = 0$$

$$x = 0, \quad C = C_i$$

$$x \to \infty, C = 0.$$

The solution is most easily achieved via Laplace transformation:

$$s\bar{C} = D_V \frac{d^2\bar{C}}{dx^2} \quad (t = 0 \text{ used}) \qquad (A.3)$$

$$x = 0, \quad \bar{C} = \frac{C_i}{s}$$

$$x \to \infty, \bar{C} \to 0 .$$

The solution in the Laplace domain is:

$$\bar{C} = A \exp\left(- \sqrt{\frac{s}{D_V}} x \right) + B \exp\left(\sqrt{\frac{s}{D_V}} x \right) \qquad (A.4)$$

$$x \to \infty \quad \Rightarrow \quad B = 0$$

$$x = 0 \quad \Rightarrow \quad A = \frac{C_i}{s}$$

$$\tilde{C} = \frac{C_i}{s}\exp\left(-\sqrt{\frac{s}{D_V}}\,x\right) \tag{A.5}$$

and the output flux is:

$$-D_V\left(\frac{d\tilde{C}}{dx}\right)_{x=0} = C_i\sqrt{\frac{D_V}{s}} \tag{A.6}$$

or, in the time domain:

$$-D_V\left(\frac{\partial C}{\partial x}\right)_{x=0} = C_i\sqrt{\frac{D_V}{\pi t}} \tag{A.7}$$

giving the mean output flux

$$\frac{1}{t_k}\int_0^{t_k} C_i\sqrt{\frac{D_V}{\pi t}}\,dt = C_i\sqrt{\frac{4D_V}{\pi t_k}} \tag{A.8}$$

or

$$J = \varepsilon_f A_{out}\left(\frac{4D_V}{\pi t_k}\right)^{1/2} C_i \ . \tag{A.9}$$

List of SKB reports

Annual Reports

1977-78
TR 121
KBS Technical Reports 1 – 120
Summaries
Stockholm, May 1979

1979
TR 79-28
The KBS Annual Report 1979
KBS Technical Reports 79-01 – 79-27
Summaries
Stockholm, March 1980

1980
TR 80-26
The KBS Annual Report 1980
KBS Technical Reports 80-01 – 80-25
Summaries
Stockholm, March 1981

1981
TR 81-17
The KBS Annual Report 1981
KBS Technical Reports 81-01 – 81-16
Summaries
Stockholm, April 1982

1982
TR 82-28
The KBS Annual Report 1982
KBS Technical Reports 82-01 – 82-27
Summaries
Stockholm, July 1983

1983
TR 83-77
The KBS Annual Report 1983
KBS Technical Reports 83-01 – 83-76
Summaries
Stockholm, June 1984

1984
TR 85-01
Annual Research and Development Report 1984
Including Summaries of Technical Reports Issued during 1984. (Technical Reports 84-01 – 84-19)
Stockholm, June 1985

1985
TR 85-20
Annual Research and Development Report 1985
Including Summaries of Technical Reports Issued during 1985. (Technical Reports 85-01 – 85-19)
Stockholm, May 1986

1986
TR 86-31
SKB Annual Report 1986
Including Summaries of Technical Reports Issued during 1986
Stockholm, May 1987

1987
TR 87-33
SKB Annual Report 1987
Including Summaries of Technical Reports Issued during 1987
Stockholm, May 1988

1988
TR 88-32
SKB Annual Report 1988
Including Summaries of Technical Reports Issued during 1988
Stockholm, May 1989

1989
TR 89-40
SKB Annual Report 1989
Including Summaries of Technical Reports Issued during 1989
Stockholm, May 1990

Technical Reports
List of SKB Technical Reports 1991

TR 91-01
Description of geological data in SKB's database GEOTAB
Version 2
Stefan Sehlstedt, Tomas Stark
SGAB, Luleå
January 1991

TR 91-02
Description of geophysical data in SKB database GEOTAB
Version 2
Stefan Sehlstedt
SGAB, Luleå
January 1991

TR 91-03
1. The application of PIE techniques to the study of the corrosion of spent oxide fuel in deep-rock ground waters
2. Spent fuel degradation
R S Forsyth
Studsvik Nuclear
January 1991

TR 91-04
Plutonium solubilities
I Puigdomènech[1], J Bruno[2]
[1]Enviromental Services, Studsvik Nuclear, Nyköping, Sweden
[2]MBT Tecnologia Ambiental, CENT, Cerdanyola, Spain
February 1991

TR 91-05
Description of tracer data in the SKB database GEOTAB
SGAB, Luleå
April, 1991

TR 91-06
Description of background data in the SKB database GEOTAB
Version 2
Ebbe Eriksson, Stefan Sehlstedt
SGAB, Luleå
March 1991

TR 91-07
Description of hydrogeological data in the SKB's database GEOTAB
Version 2
Margareta Gerlach[1], Bengt Gentzschein[2]
[1]SGAB, Luleå
[2]SGAB, Uppsala
April 1991

TR 91-08
Overview of geologic and geohydrologic conditions at the Finnsjön site and its surroundings
Kaj Ahlbom[1], Sven Tirén[2]
[1]Conterra AB
[2]Sveriges Geologiska AB
January 1991

TR 91-09
Long term sampling and measuring program. Joint report for 1987, 1988 and 1989. Within the project: Fallout studies in the Gideå and Finnsjö areas after the Chernobyl accident in 1986
Thomas Ittner
SGAB, Uppsala
December 1990

TR 91-10
Sealing of rock joints by induced calcite precipitation. A case study from Bergeforsen hydro power plant
Eva Hakami[1], Anders Ekstav[2], Ulf Qvarfort[2]
[1]Vattenfall HydroPower AB
[2]Golder Geosystem AB
January 1991

TR 91-11
Impact from the disturbed zone on nuclide migration – a radioactive waste repository study
Akke Bengtsson[1], Bertil Grundfelt[1], Anders Markström[1], Anders Rasmuson[2]
[1]KEMAKTA Konsult AB
[2]Chalmers Institute of Technology
January 1991

TR 91-12
Numerical groundwater flow calculations at the Finnsjön site
Björn Lindbom, Anders Boghammar, Hans Lindberg, Jan Bjelkås
KEMAKTA Consultants Co, Stockholm
February 1991

TR 91-13
Discrete fracture modelling of the Finnsjön rock mass
Phase 1 feasibility study
J E Geier, C-L Axelsson
Golder Geosystem AB, Uppsala
March 1991

TR 91-14
Channel widths
Kai Palmqvist, Marianne Lindström
BERGAB-Berggeologiska Undersökningar AB
February 1991

TR 91-15
Uraninite alteration in an oxidizing environment and its relevance to the disposal of spent nuclear fuel
Robert Finch, Rodney Ewing
Department of Geology, University of New Mexico
December 1990

TR 91-16
Porosity, sorption and diffusivity data compiled for the SKB 91 study
Fredrik Brandberg, Kristina Skagius
Kemakta Consultants Co, Stockholm
April 1991

TR 91-17

Seismically deformed sediments in the Lansjärv area, Northern Sweden

Robert Lagerbäck

May 1991

TR 91-18

Numerical inversion of Laplace transforms using integration and convergence acceleration

Sven-Åke Gustafson
Rogaland University, Stavanger, Norway

May 1991